

Response to Reviewer #2:

The manuscript by Jing Wei et al. presents [charger-]CPMA-SP2 measurements, from which measurements of the distribution of rBC fraction can be inferred. The manuscript is carefully written and shows that the authors have thought carefully about the interpretation of their results. The literature context is good, and the data set represents a significant contribution to the literature. However, there is one major gap which must be addressed before this manuscript is published (multiple charge correction) and another big opportunity for improvement (compare the SP2 with the analytical grade nephelometers, not only with the SP2-LEO analysis). There are also a few smaller opportunities for improvement, described below.

[Comment 1] The major gap is that this work does not cite, nor implement, the advances in [charger-]CPMA-SP2 data inversion which have been published since the original work by Liu et al., 2017 (cited by the authors). Those advances have been published in a series of papers, most recently Naseri et al. 2024, which are accompanied by open-source code for performing the calculations. The key feature of these calculations is to acknowledge the aerosol bipolar charger, which is necessarily placed before the CPMA to make sense of its output. Without this charger, the SP2 would see a large fraction of neutral particles downstream of the CPMA. With this charger, the SP2 would see not only the desired particles ($q=1$, the CPMA setpoint) but also a large fraction of doubly ($q=2$) and triply ($q=3$) charged particles. The purpose of the CPMA-SP2 data inversion code cited above is the account for these $q>1$ particles. For example, if the CPMA was set to 2 fg/e (2 femtograms per charge) and the SP2 observed a particle with 1 fg of rBC, that particle might be a 50%/50% rBC/coating particle ($q=1$, 2fg/1e), a 25%/75% rBC/coating particle ($q=2$, 4fg/2e), or even a 16% rBC (6fg/3e). A full data inversion will account for this.

Implementing this data inversion would affect:

- Eq 1, the authors write "without any assumptions", but there is an assumption of singly charged particles.
- All figures, which currently do not distinguish "doubly charged particle with BC fraction 0.5" from "singly charged particle with half the coating".

Response: We thank the reviewer for this comment. We would like to clarify that the influence of multiply charged particles ($q > 1$) has been explicitly considered in our CPMA-SP2 measurements. An X-ray aerosol neutralizer (TSI 3088) was installed upstream of the CPMA to charge the aerosols before entering the classifier (Lines 120-123). Although we did not directly use the inversion code from Liu et al. (2017a) or Naseri et al. (2024), we have applied an independent multiple charge correction procedure to the data, allowing us to identify and select only singly charged particles. All relevant details had already been included in Text S1 and Figure S10 and Figure S11. Besides, we have now explicitly stated the assumption of singly charged particles before Eq. 1 in the revised manuscript (Lines 176-178).

To facilitate readers' understanding of the data correction procedures and the CPMA–SP2 system configuration, we have added the relevant descriptions in the Methods (Lines 135-138) and Text S1 and included the aerosol neutralizer in the schematic diagram of Figure S1.

Lines 120-123: *"In this setup, particles with known mass (M_p) selected by CPMA were injected into the SP2. An X-ray aerosol neutralizer (TSI 3088) was installed upstream of the CPMA to charge the*

aerosols to a Boltzmann equilibrium before entering the classifier.”

Lines 176-178: “Under the assumption of singly charged particles, the mixing state of a single BC-containing particle can be represented by the mass ratio of the BC coating to the BC core, without relying on assumptions about particle morphology or coating structure,”

Lines 135-138: “In the subsequent data processing, measurements from the CPMA-SP2 system were first corrected for multiple charging effects. Additional corrections, including transfer function, detection efficiency, and time delay, were also applied, as detailed in the Text S1.”

Other major comments

[Comment 2] The MAC vs M_R plot of Figure S6 shows that MAC did not increase even at M_R of 5.5. Mie theory and lab experiments show that coated soot has E_{abs} 2.0 at M_R of 5.5 (Cappa et al., 2012; doi:10.1126/science.1223447). So the fundamental premise of this paper seems to be violated by Figure S6.

Response: We thank the reviewer for this comment. We would like to clarify that the MAC vs. M_R relationship in Figure S6 reflects ambient measurements under real atmospheric conditions, which are more complex than idealized laboratory experiments or theoretical Mie calculations. In the atmosphere, factors such as particle mixing state, coating composition, hygroscopic growth, and measurement uncertainties can influence the observed MAC values. Thus, the lack of further MAC enhancement beyond $M_R=5$ in our field measurement does not violate laboratory findings.

[Comment 3] The abstract claims a morphology dependent correction scheme but none of the data are morphology dependent. The introduction could be enhanced by adding a discussion of how morphology can be measured. Or, the word morphology could be removed from the final paragraph. I suggest removing it, as the true measurement here is M_R , not morphology.

Response: We thank the reviewer for this constructive comment and agree that references to particle morphology were not appropriate. All morphology-related descriptions have been removed from the Abstract and main text. These statements have been revised to explicitly describe M_R -dependent optical transition behavior, rather than particle morphology. We believe these changes improve the accuracy and clarity of the revised manuscript.

[Comment 4] Line 154, the MAC of 9 m²/g is 3 standard deviations than the expected value of 8 ± 0.7 m²/g at 550 nm (Liu et al 2020). Please comment.

Response: We thank the reviewer for this comment. The reported MAC of 9.08 m²/g corresponds to pure BC, representing the intrinsic light absorption efficiency of BC without the influence of any coating materials. Therefore, this value is independent of the mixing state and reflects the inherent optical property of BC itself. The slightly higher value compared to the expected 8 ± 0.7 m²/g at 550 nm (Liu et al., 2020) can be attributed to several plausible factors. (1) BC morphology: even for uncoated BC, variations in aggregate compactness, fractal dimension, and cluster structure can modulate light absorption efficiency. (2) Instrumental and calibration effects: Differences in SP2 calibration with Aquadag standards, detector response, and limited sampling statistics can cause small biases in the retrieved MAC. Overall, the measured MAC of pure BC in this study is considered more representative of the local BC characteristics under actual atmospheric conditions.

In response to similar comments from other reviewers, we have also added a brief note in the main manuscript to clarify these uncertainties (Lines 219-228).

“The $MAC_{BC_core_measured}$ at wavelength of 630 nm was $9.08 \pm 0.53 \text{ m}^2 \text{ g}^{-1}$ (mean \pm 90% confidence Interval) (Fig. S6). Based on our error propagation analysis, which accounts for measurement uncertainties in particle absorption and BC mass as well as the standard error of the extrapolation, the estimated uncertainty of $MAC_{BC_core_measured}$ is approximately 19-23% (Text S2). And the uncertainty of $E_{abs_measured}$ is approximately 26 - 32% (Text S2). For comparison, the $MAC_{BC_core_measured}$ is slightly higher than the value of $7.5 \text{ m}^2 \text{ g}^{-1}$ recommended by Bond and Bergstrom (2006) but still within the range reported by other study ($\sim 6.5 - 17 \text{ m}^2 \text{ g}^{-1}$) (Zanatta et al., 2016), likely due to variations in measurement methods, and site-specific atmospheric conditions.”

[Comment 5] Figure 3: Is the positive correlation truly statistically significant? Please use prediction bands and add uncertainty in the fit coefficient. Is it truly different from 1? It seems to me that there is not a significant relationship.

Response: We appreciate the reviewer’s comment. We have re-examined the correlation between the measured and modeled scattering cross-sections and performed a statistical significance test for the fitted slope. The P-value of the regression coefficient is less than 0.05, indicating that the positive correlation is statistically significant. In addition, we have added the 95% prediction bands and the uncertainty of the fitted slope in Figure 3 to better illustrate the confidence range of the relationship. We hope that these additional analyses and revisions provide a more complete and convincing presentation of the relationship.

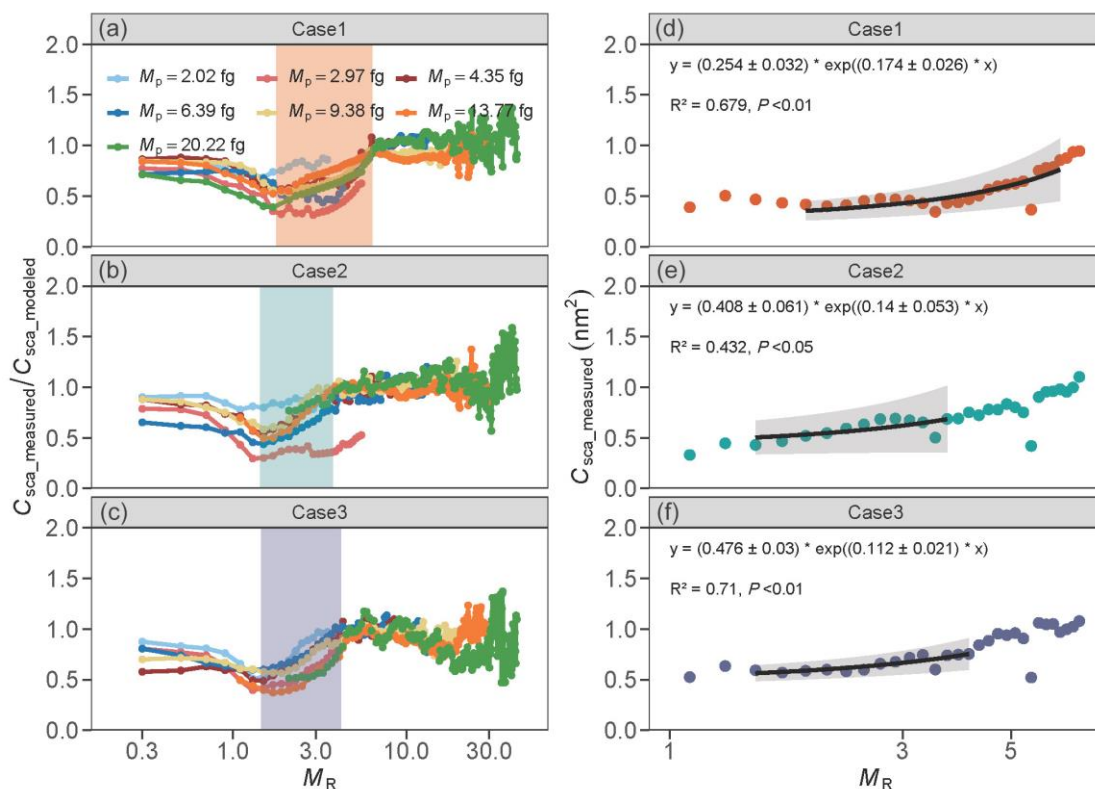


Figure. 3 The optical behavior of BC-containing particles as a function of mass ratio (coating-to-

BC , M_R). (a) – (c) show the ratio of measured to modeled scattering cross-section at the wavelength of 1064 nm during different cases. The shadows indicate the M_R ranges corresponding to “transition-state” BC-containing particles. (d) – (f) present the measured scattering cross-section as a function of M_R , along with fitted optical transition-dependent models representing the “transition-state” BC-containing particles. The fitted curves include the corresponding P-values, and the shaded areas denote the 95% confidence intervals.

[Comment 6] Line 181 why not model the nephelometer instead of the SP2? You have already assumed a wavelength independent rBC refractive index.

Response: We appreciate the reviewer’s suggestion. However, the nephelometer measures the bulk scattering coefficient of all particles in the ambient, rather than the scattering cross section (C_{sca}) of BC-containing particles. In contrast, the SP2 provides single-particle information, allowing us to quantify the scattering cross section of individual BC-containing particles. Our goal in this study is to establish the relationship between the measured and modeled C_{sca} of BC-containing particles as a function of the M_R , which reflects M_R -dependent optical transition behavior during BC aging. Therefore, only SP2-derived single-particle C_{sca} are suitable for this analysis, while nephelometer measurements cannot serve this purpose. In this work, the nephelometer data were used only to compare with the CAPS measurements to evaluate the accuracy of the CAPS-derived scattering coefficients.

[Comment 7] Figure 4 shows “E_abs,improved” but this paper does not actually demonstrate an improvement. The results here do not seem generalizable. Rename to “E_abs,this work”

Response: We thank the reviewer for the suggestion. We agree that the term “E_abs, improved” may overstate the generality of our results. However, since the parameter represents the E_{abs} derived from our refined modeling approach, we have renamed it as “ E_{abs_param} ” throughout the text and Figure 4. This revised label more accurately reflects that it is based on an improved method rather than implying universally better performance.

Minor comments

[Comment 8] Line 56, you might cite Radney et al. 2014 and Corbin et al. 2023.

Response: We thank the reviewer for the helpful suggestion. The references Radney et al. (2014) and Corbin et al. (2023) have been added at Lines 70 to support the corresponding statement.

[Comment 9] Line 58, please cite a paper for “or located on the particle surface” or for the entire sentence.

Response: We thank the reviewer for the suggestion. The statement has been supported by appropriate references, and Zhang et al. (2008) and Adachi and Buseck (2013) have been added accordingly. (Lines 70-72)

“Early aging stage feature uneven coatings, while aged particles show BC core either encapsulated or located near the particle surface (Zhang et al., 2008; Adachi and Buseck, 2013).”

[Comment 10] Line 99, “noisy scattering signals” or “noisy incandescence signals”? The section is discussing M_R ? Please also explain “noisy” with a few more words.

Response: We thank the reviewer for the comment. The sentence has been clarified to specify that the exclusion was based on noisy scattering signals, which were caused by weak signal intensity and low signal-to-noise ratio for small particles. The corresponding revision has been made in the revised manuscript. (Lines 130-133)

“During further data analysis, particles with $M_p = 0.93$ fg and $M_p = 1.37$ fg exhibited excessively noisy scattering signals, likely due to weak signal intensity and low signal-to-noise ratio for small particles, and were therefore excluded from subsequent statistical analysis.”

[Comment 11] Line 103, does this aquadag correction factor trace back to Gysel et al. (2011)? Either way, that early paper should be cited.

Response: We thank the reviewer for the helpful suggestion. The Aquadag correction factor used in this study is mainly based on the approach described by Liu et al. (2014) while Gysel et al. (2011) is now also cited to acknowledge the original development of this correction method. Both references have been added at Line 138-141 in the revised manuscript.

“The mass of each BC core (M_{BC_core}) was then calculated from the SP2 incandescence signal using the calibration described above, with a correction factor of 0.75 applied to the peak height (Liu et al., 2020; Liu et al., 2014; Zhang et al., 2018; Gysel et al., 2011).”

[Comment 12] Line 124, why compare 2 difference averaging times?

Response: We thank the reviewer for the helpful comment. The detection limits of the Nephelometer and CAPS were reported according to their respective instrument specifications, which use different default averaging times. Our intention was not to directly compare the two instruments, but only to indicate their detection limits. This clarification has been added to the revised manuscript (Lines 171-173).

“The lower detection limit of the Nephelometer at all three wavelengths was 0.3 Mm^{-1} with a 60-second integration time, while that of the CAPS-ALB was 1 Mm^{-1} with 30-second integration time.”

[Comment 13] Line 125, Did you calibrate the CAPS extinction measurement with this scattering calibration?

Response: We thank the reviewer for this question. We thank the reviewer for this question. The CAPS extinction channel was not directly calibrated using the PSL scattering calibration. The CAPS was calibrated following the manufacturer-recommended procedure, in which extinction is referenced to Rayleigh scattering by filtered air. For monodisperse PSL particles, the optical extinction is theoretically equal to the scattering because PSL is a purely scattering aerosol. Therefore, the PSL-based scattering calibration was used as an independent verification of the CAPS extinction response rather than as its primary calibration. The good agreement between PSL-derived scattering (equivalent to extinction for PSL) and the CAPS extinction measurement confirms the accuracy and wavelength consistency of the CAPS calibration (Figure R1).

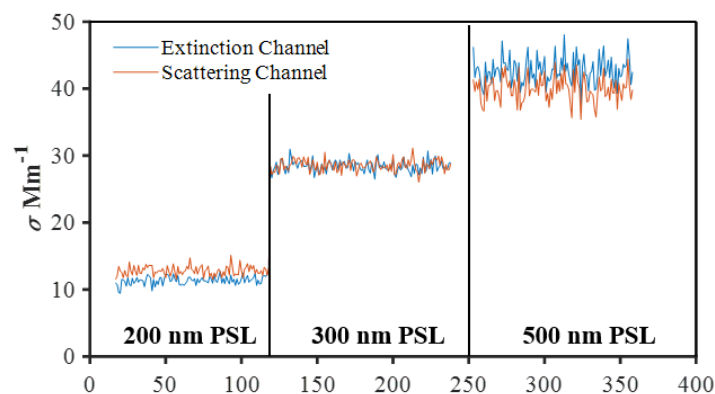


Figure R1. PSL-derived scattering versus CAPS extinction measurements during PSL injection.

[Comment 14] Line 137, this refractive index is very precise (1.48) would you not expect variability (1.5 to 1.6?). Also, a different RI is cited later on line 164.

Response: We thank the reviewer for this comment. In the revised manuscript, we have clarified the use of refractive indices in relation to the M_R -dependent optical transition behavior of BC-containing particles. At Line 137, the refractive indices were selected specifically for deriving the M_R -dependent optical transition behavior from SP2 scattering measurements at 1064 nm. The BC core is assigned a complex refractive index of 2.26-1.26i, while the non-absorbing coating has a refractive index of 1.48 and a density of 1.5 g cm⁻³, values that have been widely used in previous studies (Liu et al., 2017a; Zhao et al., 2020; Liu et al., 2015). Besides, since the coating in this work does not absorb at 1064 nm, its absorption can be safely ignored for determining scattering and transition characteristics. In contrast, at line 164, our analysis focuses on calculating E_{abs} at 630 nm, consistent with the CAPS measurement wavelength. We apologize for the confusion caused by the earlier description. We have now clarified and reorganized the wavelength-specific assumptions and the M_R -dependent optical transition behavior in the revised manuscript (Lines 189-200 and Lines 235-239):

Lines 190-200: “The M_R -dependent optical transitions of BC-containing particles were further derived from SP2 measurements at a wavelength of 1064 nm. In the CPMA-SP2 system, when both M_p and M_{BC_core} are known, the modeled scattering cross section ($C_{sca_modeled}$) of BC-containing particles can be derived using Mie theory (Wang et al., 2021). This calculation assumes a core-shell structure, with the BC core having a refractive index of 2.26-1.26i (Liu et al., 2017a; Zhao et al., 2020) and the non-absorbing coating characterized by a refractive index of 1.48 and a density of 1.5 g cm⁻³ at a wavelength of 1064 nm (Liu et al., 2015). The measured scattering cross section ($C_{sca_measured}$) was obtained from the SP2 using the leading-edge-only (LEO) technique, which reconstructs the scattering signal as BC-containing particles pass through the SP2 laser beam due to partial evaporation of refractory-absorbing material.”

Lines 236-240: “Given the measurement data available in this study, the Core-shell Mie theory was used to calculate the E_{abs} of BC-containing particles at a wavelength of 630 nm. The refractive index (RI) of BC and its coatings are assumed to be $n=1.85+0.71i$ and $n=1.5+0i$ at a wavelength of 630 nm (Liu et al., 2015; Liu et al., 2014).”

[Comment 15] Line 157, please add Generalized Mie Model to the list.

Response: We thank the reviewer for the suggestion. The Generalized Mie Model has been added to the list of commonly used models for calculating the optical properties of BC-containing particles (Line 232).

[Comment 16] Several examples: Please change "(Method)" to a section reference.

Response: We thank the reviewer for the suggestion. All instances of "(Method)" have been updated to refer to the specific section, Section 2.2, in the revised manuscript (Line 242).

[Comment 17] Line 181, mathematical -> empirical

Response: Corrected.

[Comment 18] Line 255-256, is there any experimental evidence to quantify the M_R the rBC would become fully embedded?

Response: We thank the reviewer for raising this important question. In the revised manuscript, we no longer describe the embedding of BC cores. Instead, following the reviewer's comment and consistent with several other related suggestions, we have thoroughly rewritten this part of the text. In the updated analysis, the ratio of $C_{sca_measured}/C_{sca_modeled}$ derived from SP2 measurements and core-shell Mie calculations is treated as an optical proxy that indirectly reflects the M_R -dependent optical transition behavior of BC-containing particles. This ratio is used to infer changes in particle compaction and coating state based solely on optical responses, rather than to identify a precise experimental M_R value corresponding to full embedding. As now clarified, the transition ranges reported in the manuscript represent optically inferred transition states, not morphologically observed boundaries (Lines 346-373)

"The SP2 measures the scattering cross-section (C_{sca}) of single BC-containing particles. The comparison between measured and the modeled (by Core-shell Mie model) C_{sca} serves as an optical proxy of changes in BC compaction and coating state, reflecting the evolution of optical properties during aging process. Fig. 3 presents the variation of the ratio $C_{sca_measured}/C_{sca_modeled}$ at wavelength of 1064 nm with M_R under different M_p . When M_R is relatively low, $C_{sca_measured}/C_{sca_modeled}$ is less than 1, suggesting that the BC cores may exist in a fractal structure, remain bare, or are not fully embedded in the coating materials. Consequently, the measured C_{sca} is lower than the C_{sca} predicted by the core-shell Mie model. This observation aligns with Liu et al. (2017a), who classified such BC-containing particles as externally mixed. As M_R increases, $C_{sca_measured}/C_{sca_modeled}$ also increases, indicating the BC particles becomes more compact and more thoroughly coated, transitioning toward a core-shell structure (Corbin et al., 2023). Following previous studies (Liu et al., 2017a; Liu et al., 2020), we describe this stage as a "transition state". In this work, the transition state is neither defined by a fixed M_R threshold nor by any directly observed morphological boundary. Instead, it reflects an optically inferred state in which scattering enhancement increases markedly, with M_R ranges of 1.78-6.34 (Case 1), 1.43-3.78 (Case 2), and 1.45-4.19 (Case 3). The higher M_R thresholds observed in Case 2 and Case 3 indicate that under polluted conditions, BC particles can reach an optically core-shell-like state with comparatively less coating material. This likely reflected accelerated aging driven by enhanced secondary formation and condensation of inorganics and organics on BC, facilitated by stagnant meteorological conditions (low wind speed). Such conditions promote efficient coating growth on BC-containing particles, strengthening their light-absorption capability and leading to high E_{abs} . Therefore, compared with Case 1, BC in Case 2 and

Case 3 required less coating material to reach the core-shell configuration. When M_R exceeds the transition state range, the ratio $C_{sca_measured}/C_{sca_modeled}$ becomes relatively stable, suggesting that the BC particles behave optically like compact, spherical core-shell structures.”

[Comment 19] Figure S1, CPAS not defined. ACSM not defined. Define all acronyms in caption.

Response: We appreciate the reviewer’s comment. As all instrument acronyms are listed and defined in Table S1, we prefer not to repeat them in each figure caption to avoid redundancy.

[Comment 20] Line 323, "during the haze period... chemical reactions produced a large number of inorganic substances..." How do you know this?

Response: We thank the reviewer for the comment. As this point was also raised by **reviewer 1 [Comment 31]**, we have provided a detailed clarification in our previous response. Briefly, the relevant section has been thoroughly revised to remove unsupported statements and to base the discussion solely on our measured chemical composition data. The updated analysis shows that only secondary nitrate exhibits a consistent association with increasing $E_{abs_measured}$, while other inorganic and organic components do not show significant effects. This revised, data-driven interpretation is now fully reflected in the revised manuscript (Lines 415-457).

“The transitional-state particles are BC-containing particles in the process of evolving from loosely aggregated fractal-like structures toward quasi-core-shell configurations (Moffet et al., 2016; Moteki and Kondo, 2007). The abundance of transitional-state particles varies notably under different atmospheric conditions, directly influencing the measured E_{abs} (Liu et al., 2017a). During clean days (Case 1), the atmospheric environment was characterized by low PM_{10} concentrations, weak secondary formation, and highly variable coating conditions. Under such conditions, our measurements show that BC-containing particles were dominated by transitional-state structures (Fig. S9), representing the intermediate stage between externally mixed aggregates and fully developed quasi-core-shell structures. The limited and heterogeneous coating distribution on these particles substantially weakens the lensing effect, resulting in lower measured E_{abs} (Peng et al., 2016). Because the core-shell Mie model inherently assumes a uniform and concentric coating, it does not accurately represent the optical behavior of these transitional particles, leading to a pronounced overestimation of measured E_{abs} during Case 1. This indicates that, under clean conditions, the optical properties of transitional-state particles are the key driver of the model-observation discrepancy. In contrast, the haze period (Case 2) represents a more aged and heavily coated aerosol environment and provides a useful reference for understanding the factors influencing the measured E_{abs} . During Case 2, the high aerosol loading and elevated bulk-averaged M_R were largely influenced by regional transport, as air masses at 100 m, 500 m, and 1000 m all followed similar pathways from the northern Yangtze River Delta into northern Zhejiang (Fig. 1c and Fig. S7). Stagnant meteorological conditions, elevated relative humidity, and enhanced oxidative capacity further facilitated vigorous liquid-phase and photochemical reactions, promoting the abundant formation of secondary coatings on BC surfaces (Peng et al., 2016). Notably, our observations show that E_{abs} increases systematically with the increasing contribution of secondary nitrate (Fig. S8), consistent with the fact that nitrate-rich conditions enhance aqueous-phase oxidation and accelerate the formation of thick inorganic coatings (Liu et al., 2017b). As a result, a much larger fraction of BC-containing particles exhibited internally mixed, quasi-core-shell structures rather than transitional states (Fig. S9), which explains why the core-shell Mie model

performs substantially better for Case 2 than for Case 1. This contrast reinforces the central role of transitional-state particles in determining measured E_{abs} when coatings are sparse, irregular, or partially developed. Given the strong influence of transitional-state particles on measured E_{abs} in Case 1, precise constraints on their optical behavior are crucial for improving E_{abs} estimates across different atmospheric scenarios. To address this, an empirical formula based on optical measurements was developed to estimate the E_{abs} of BC-containing particles in the “transition state”, derived from fitting the measured C_{sca} against M_R (Fig. 3d-3f). By applying this empirical formula to the calculation of E_{abs} , the resulting value for Case 1 was 1.21 ± 0.01 . For Case 2 and Case 3, the E_{abs} calculated using the same formula (E_{abs_param}) remained slightly lower than the $E_{abs_measured}$, but the deviation was within 20%, demonstrating the reliability of the approach across different atmospheric conditions.”

[Comment 21] Line 327, please define "embedding pattern"

Response: We thank the reviewer for this comment. In response to this and related reviewer suggestions, we have removed the term “embedding pattern” and substantially revised this section to avoid implying any morphology-based classification that cannot be directly observed. The revised text now focuses on the concept of transitional-state BC-containing particles, defined solely based on their M_R -dependent optical transition behavior inferred from SP2 measurements and Mie-model calculations. The updated description is provided in Lines 415-419 of the revised manuscript.

“The transitional-state particles are BC-containing particles in the process of evolving from loosely aggregated fractal-like structures toward quasi–core–shell configurations (Moffet et al., 2016; Moteki and Kondo, 2007). The abundance of transitional-state particles varies notably under different atmospheric conditions, directly influencing the measured E_{abs} (Liu et al., 2017a).”

[Comment 22] Line 331, either the formation of BC coatings was "unfavourable" or the plume was less aged.

Response: We thank the reviewer for this comment. In response, and taking into account similar feedback from other reviewers, we have thoroughly revised this section to clarify the roles of coating formation conditions and plume aging. The discussion now avoids unsupported statements and provides a more data-driven interpretation (see Lines 415-457 in the revised manuscript).

“The transitional-state particles are BC-containing particles in the process of evolving from loosely aggregated fractal-like structures toward quasi–core–shell configurations (Moffet et al., 2016; Moteki and Kondo, 2007). The abundance of transitional-state particles varies notably under different atmospheric conditions, directly influencing the measured E_{abs} (Liu et al., 2017a). During clean days (Case 1), the atmospheric environment was characterized by low PM_{10} concentrations, weak secondary formation, and highly variable coating conditions. Under such conditions, our measurements show that BC-containing particles were dominated by transitional-state structures (Fig. S9), representing the intermediate stage between externally mixed aggregates and fully developed quasi–core–shell structures. The limited and heterogeneous coating distribution on these particles substantially weakens the lensing effect, resulting in lower measured E_{abs} (Peng et al., 2016). Because the core-shell Mie model inherently assumes a uniform and concentric coating, it does not accurately represent the optical behavior of these transitional particles, leading to a pronounced overestimation of measured E_{abs} during Case 1. This indicates that, under clean

conditions, the optical properties of transitional-state particles are the key driver of the model-observation discrepancy. In contrast, the haze period (Case 2) represents a more aged and heavily coated aerosol environment and provides a useful reference for understanding the factors influencing the measured E_{abs} . During Case 2, the high aerosol loading and elevated bulk-averaged M_R were largely influenced by regional transport, as air masses at 100 m, 500 m, and 1000 m all followed similar pathways from the northern Yangtze River Delta into northern Zhejiang (Fig. 1c and Fig. S7). Stagnant meteorological conditions, elevated relative humidity, and enhanced oxidative capacity further facilitated vigorous liquid-phase and photochemical reactions, promoting the abundant formation of secondary coatings on BC surfaces (Peng et al., 2016). Notably, our observations show that E_{abs} increases systematically with the increasing contribution of secondary nitrate (Fig. S8), consistent with the fact that nitrate-rich conditions enhance aqueous-phase oxidation and accelerate the formation of thick inorganic coatings (Liu et al., 2017b). As a result, a much larger fraction of BC-containing particles exhibited internally mixed, quasi-core-shell structures rather than transitional states (Fig. S9), which explains why the core-shell Mie model performs substantially better for Case 2 than for Case 1. This contrast reinforces the central role of transitional-state particles in determining measured E_{abs} when coatings are sparse, irregular, or partially developed. Given the strong influence of transitional-state particles on measured E_{abs} in Case 1, precise constraints on their optical behavior are crucial for improving E_{abs} estimates across different atmospheric scenarios. To address this, an empirical formula based on optical measurements was developed to estimate the E_{abs} of BC-containing particles in the “transition state”, derived from fitting the measured C_{sca} against M_R (Fig. 3d-3f). By applying this empirical formula to the calculation of E_{abs} , the resulting value for Case 1 was 1.21 ± 0.01 . For Case 2 and Case 3, the E_{abs} calculated using the same formula (E_{abs_param}) remained slightly lower than the $E_{abs_measured}$, but the deviation was within 20%, demonstrating the reliability of the approach across different atmospheric conditions.”

References:

- Adachi, K. and Buseck, P. R.: Changes of ns-soot mixing states and shapes in an urban area during CalNex, *Journal of Geophysical Research-Atmospheres*, 118, 3723-3730, 10.1002/jgrd.50321, 2013.
- Bond, T. C. and Bergstrom, R. W.: Light Absorption by Carbonaceous Particles: An Investigative Review, *Aerosol Science and Technology*, 40, 27-67, 10.1080/02786820500421521, 2006.
- Corbin, J. C., Modini, R. L., and Gysel-Beer, M.: Mechanisms of soot-aggregate restructuring and compaction, *Aerosol Science and Technology*, 57, 89-111, 10.1080/02786826.2022.2137385, 2023.
- Gysel, M., Laborde, M., Olfert, J. S., Subramanian, R., and Gröhn, A. J.: Effective density of Aquadag and fullerene soot black carbon reference materials used for SP2 calibration, *Atmospheric Measurement Techniques*, 4, 2851-2858, 10.5194/amt-4-2851-2011, 2011.
- Liu, D., Taylor, J. W., Young, D. E., Flynn, M. J., Coe, H., and Allan, J. D.: The effect of complex black carbon microphysics on the determination of the optical properties of brown carbon: BC morphology on BrC optical properties, *Geophysical Research Letters*, 42, 613-619, 10.1002/2014GL062443, 2015.
- Liu, D., Allan, J. D., Young, D. E., Coe, H., Beddows, D., Fleming, Z. L., Flynn, M. J., Gallagher, M. W., Harrison, R. M., Lee, J., Prevot, A. S. H., Taylor, J. W., Yin, J., Williams, P. I., and Zotter, P.: Size distribution, mixing state and source apportionment of black carbon aerosol in London during

- wintertime, *Atmospheric Chemistry and Physics*, 14, 10061-10084, 10.5194/acp-14-10061-2014, 2014.
- Liu, D., Whitehead, J., Alfarra, M. R., Reyes-Villegas, E., Spracklen, D. V., Reddington, C. L., Kong, S., Williams, P. I., Ting, Y.-C., Haslett, S., Taylor, J. W., Flynn, M. J., Morgan, W. T., McFiggans, G., Coe, H., and Allan, J. D.: Black-carbon absorption enhancement in the atmosphere determined by particle mixing state, *Nature Geoscience*, 10, 184-188, 10.1038/ngeo2901, 2017a.
- Liu, H., Pan, X., Liu, D., Liu, X., Chen, X., Tian, Y., Sun, Y., Fu, P., and Wang, Z.: Mixing characteristics of refractory black carbon aerosols at an urban site in Beijing, *Atmospheric Chemistry and Physics*, 20, 5771-5785, 10.5194/acp-20-5771-2020, 2020.
- Liu, Y., Wu, Z., Wang, Y., Xiao, Y., Gu, F., Zheng, J., Tan, T., Shang, D., Wu, Y., Zeng, L., Hu, M., Bateman, A. P., and Martin, S. T.: Submicrometer Particles Are in the Liquid State during Heavy Haze Episodes in the Urban Atmosphere of Beijing, China, *Environmental Science & Technology Letters*, 4, 427-432, 10.1021/acs.estlett.7b00352, 2017b.
- Moffet, R. C., O'Brien, R. E., Alpert, P. A., Kelly, S. T., Pham, D. Q., Gilles, M. K., Knopf, D. A., Laskin, A., Pacific Northwest National Lab, R. W. A. E. M. S. L., Lawrence Berkeley National Lab, B. C. A., and Stony Brook Univ, S. B. N. Y.: Morphology and mixing of black carbon particles collected in central California during the CARES field study, *Atmospheric chemistry and physics*, 16, 14515-14525, 10.5194/acp-16-14515-2016, 2016.
- Moteki, N. and Kondo, Y.: Effects of Mixing State on Black Carbon Measurements by Laser-Induced Incandescence, *Aerosol Science and Technology*, 41, 398-417, 10.1080/02786820701199728, 2007.
- Naseri, A., Corbin, J. C., and Olfert, J. S.: Comparison of the LEO and CPMA-SP2 techniques for black-carbon mixing-state measurements, *Atmos. Meas. Tech.*, 17, 3719-3738, 10.5194/amt-17-3719-2024, 2024.
- Peng, J., Hu, M., Guo, S., Du, Z., Zheng, J., Shang, D., Zamora, M. L., Zeng, L., Shao, M., Wu, Y.-S., Zheng, J., Wang, Y., Glen, C. R., Collins, D. R., Molina, M. J., and Zhang, R.: Markedly enhanced absorption and direct radiative forcing of black carbon under polluted urban environments, *Proceedings of the National Academy of Sciences*, 113, 4266-4271, 10.1073/pnas.1602310113, 2016.
- Radney, J. G., You, R. A., Ma, X. F., Conny, J. M., Zachariah, M. R., Hodges, J. T., and Zangmeister, C. D.: Dependence of Soot Optical Properties on Particle Morphology: Measurements and Model Comparisons, *Environmental Science & Technology*, 48, 3169-3176, 10.1021/es4041804, 2014.
- Wang, T. T., Zhao, G., Tan, T. Y., Yu, Y., Tang, R. Z., Dong, H. B., Chen, S. Y., Li, X., Lu, K. D., Zeng, L. M., Gao, Y. Q., Wang, H. L., Lou, S. R., Liu, D. T., Hu, M., Zhao, C. S., and Guo, S.: Effects of biomass burning and photochemical oxidation on the black carbon mixing state and light absorption in summer season, *Atmospheric Environment*, 248, 10.1016/j.atmosenv.2021.118230, 2021.
- Zanatta, M., Gysel, N., Bukowiecki, T., Müller, E., and Weingartner: A European aerosol phenomenology-5: Climatology of black carbon optical properties at 9 regional background sites across Europe, *Atmospheric Environment*, 2016.
- Zhang, R. Y., Khalizov, A. F., Pagels, J., Zhang, D., Xue, H. X., and McMurry, P. H.: Variability in morphology, hygroscopicity, and optical properties of soot aerosols during atmospheric processing, *Proc. Natl. Acad. Sci. U. S. A.*, 105, 10291-10296, 10.1073/pnas.0804860105, 2008.
- Zhang, Y., Zhang, Q., Cheng, Y., Su, H., Li, H., Li, M., Zhang, X., Ding, A., and He, K.: Amplification of light absorption of black carbon associated with air pollution, *Atmospheric Chemistry and Physics*, 18, 9879-9896, 10.5194/acp-18-9879-2018, 2018.

Zhao, G., Shen, C., and Zhao, C.: Technical note: Mismeasurement of the core-shell structure of black carbon-containing ambient aerosols by SP2 measurements, *Atmospheric Environment*, 243, 117885, 10.1016/j.atmosenv.2020.117885, 2020.